Neuropharmacology 123 (2017) 1–9

Contents lists available at ScienceDirect

Neuropharmacology

journal homepage: www.elsevier.com/locate/neuropharm

Neuropharmacological characterization of the new psychoactive substance methoxetamine

Laura Hondebrink [a, 1], Emma E.J. Kasteel [a, b, 1], Anke M. Tukker [b], Fiona M.J. Wijnolts [b], Anouk H.A. Verboven [b], Remco H.S. Westerink [b, *]

[a] Dutch Poisons Information Center (DPIC), University Medical Center Utrecht, P.O. Box 85500, NL-3508 GA, Utrecht, The Netherlands
[b] Neurotoxicology Research Group, Division Toxicology, Institute for Risk Assessment Sciences (IRAS), Faculty of Veterinary Medicine, Utrecht University, P.O. Box 80.177, NL-3508, Utrecht, The Netherlands

ARTICLE INFO

Article history:
Received 13 October 2016
Received in revised form
22 April 2017
Accepted 24 April 2017
Available online 25 April 2017

Chemical compounds studied in this article:
Methoxetamine (PubChem CID: 52911279)
Ketamine (PubChem CID: 44632368)

Keywords:
Methoxetamine
Ketamine
Human induced pluripotent stem cell-derived neurons
Neuronal electrical activity
Glutamatergic neurotransmission
Monoamine transporters

ABSTRACT

The use of new psychoactive substances (NPS) is steadily increasing. One commonly used NPS is methoxetamine (MXE), a ketamine analogue. Several adverse effects have been reported following MXE exposure, while only limited data are available on its neuropharmacological modes of action.

We investigated the effects of MXE and ketamine on several endpoints using multiple *in vitro* models. These included rat primary cortical cells, human SH-SY5Y cells, human induced pluripotent stem cell (hiPSC)-derived iCell® Neurons, DopaNeurons and astrocyte co-cultures, and human embryonic kidney (HEK293) cells. We investigated effects on several neurotransmitter receptors using single cell intracellular calcium $[Ca^{2+}]_i$ imaging, effects on neuronal activity using micro-electrode array (MEA) recordings and effects on human monoamine transporters using a fluorescence-based plate reader assay.

In rat primary cortical cells, 10 μM MXE increased the glutamate-evoked increase in $[Ca^{2+}]_i$, whereas 10 μM ketamine was without effect. MXE and ketamine did not affect voltage-gated calcium channels (VGCCs), but inhibited spontaneous neuronal activity (IC_{50} 0.5 μM and 1.2 μM respectively). In human SH-SY5Y cells, 10 μM MXE slightly inhibited the K^+- and acetylcholine-evoked increase in $[Ca^{2+}]_i$. In hiPSC-derived iCell®(Dopa)Neurons, only the ATP-evoked increase in $[Ca^{2+}]_i$ was slightly reduced. Additionally, MXE inhibited spontaneous neuronal activity (IC_{50} between 10 and 100 μM). Finally, MXE potently inhibits uptake via monoamine transporters (DAT, NET and SERT), with IC_{50} values in the low micromolar range (33, 20, 2 μM respectively).

Our combined *in vitro* data provide an urgently needed first insight into the multiple modes of action of MXE. The use of different models and different (neuronal) endpoints can be complementary in pharmacological profiling. Rapid *in vitro* screening methods as those presented here, could be of utmost importance for gaining a first mechanistic insight to aid the risk assessment of emerging NPS.

1. Introduction

New psychoactive substances (NPS) are an emerging class of chemicals on the drug market. NPS are also known as 'legal highs' and mimic the psychoactive effects of illicit drugs, but are often not legislated. Over the last years, the number, type and availability of NPS is growing. In 2009, only 24 NPS were reported for the first time in Europe, increasing up to 98 additional NPS in 2015 (EMCDDA, 2016; Europol, 2013). Surveys amongst young adults showed an increase in the use of legal highs, from 5% in 2011 to 8% in 2014. In the Netherlands, 0.5% of all analyzed drug samples contained NPS in 2007, which increased to 8% in 2013 (Hondebrink et al., 2015).

In the Netherlands, methoxetamine ((RS)-2-(ethylamino)-2-(3-methoxyphenyl)cyclohexanone, MXE) was the second most frequently detected NPS in drug samples in 2013; 1.2% of all analyzed drug samples contained MXE (Hondebrink et al., 2015). In 2014, 13% of the ketamine samples offered to the Dutch Drugs Information and Monitoring System (DIMS) contained MXE (van der Gouwe, 2014). Among Dutch partygoers (15–35 years), 3% has used MXE (Linsen et al., 2015). In other countries, MXE is also a popular

* Corresponding author.
E-mail address: r.westerink@uu.nl (R.H.S. Westerink).
[1] Both authors contributed equally to this study.

http://dx.doi.org/10.1016/j.neuropharm.2017.04.035
0028-3908/

NPS with a life-time prevalence of use around 5% in the USA and the UK. Life-time prevalence of MXE use increases among ketamine users to 28% (USA) and 13% (UK) (Lawn et al., 2014).

MXE is a ketamine analogue that was sold as a 'legal' replacement for ketamine (EMCDDA-Europol, 2014). It is categorized as a hallucinogen, a class which also includes drugs like D-lysergic acid diethylamide (LSD), phencyclidine (PCP) and dextromethorphan. MXE is a dissociative anesthetic, producing derealization, sensory deprivation and dissociation from the physical body, which are all features of a 'near-death experience' and part of the desired effects of MXE (Corazza et al., 2012). Other desired effects include euphoria, feelings of peacefulness, increased empathy and social interaction and a sense of going deeper inside the self (Zawilska, 2014). These intended effects are similar to those of ketamine, but much longer lasting and with a delay in the effects (Corazza et al., 2013, 2012). As a consequence of this delay, users more frequently take a second dose, increasing the risk for adverse effects. The estimated brain concentration of MXE during recreational use is 1–5 μM (Zwartsen et al., 2017), although levels can be higher during overdose.

Multiple deaths are reported after MXE exposure, which are often associated with hyperthermia and/or the presence of other drugs of abuse (Zanda et al., 2016; Zawilska, 2014). MXE has been implicated in at least 22 fatal and 110 non-fatal intoxications, spread over eight European countries (EMCDDA and Europol, 2014; Zanda et al., 2016). MXE-induced toxicity includes psychiatric, cognitive, neurological and cardiovascular symptoms. These include drowsiness, slurred speech, anxiety, reduced ability to focus and concentrate, tremor, impaired motor coordination, aggression, hypertension and tachycardia (for review see Zawilska, 2014) as well as depressive thoughts and suicide attempts (Corazza et al., 2013).

Despite these obvious risks, the neuropharmacology of MXE is largely unknown. *In vivo* data show that MXE use is associated with bladder and renal toxicity, although MXE is advertised as a 'bladder-friendly' alternative to ketamine (Dargan et al., 2014). In rats, MXE acts as a typical dissociative anesthetic: it produces anxiogenic and stimulant effects at low doses and sedative effects at high doses. The longer lasting effects compared to ketamine described in human case reports are confirmed in rats. Moreover, MXE accumulates in the brain, which can explain the increased psychological effects (both desired and adverse) and increased toxicity compared with ketamine (Horsley et al., 2016). The limited available *in vitro* studies indicate that MXE may resemble the pharmacology of ketamine, which main mechanism is antagonism of the glutamate N-methyl-D-aspartate (NMDA) receptor (Bergman, 1999). A high binding affinity of MXE for the NMDA receptor was indeed reported (K_i 259 nM, Roth et al., 2013). While MXE also has high binding affinity for the human serotonin transporter (hSERT, Ki 0.5 μM), ketamine did not show binding affinity for hSERT at 10 μM (Roth et al., 2013). However, data demonstrating modulation of transporter or receptor function are not yet available.

Although data on the pharmacological profile of MXE are limited, human exposure and (severe) adverse effects continue to occur. Consequently, it is of importance to gain insight in the modes of action and neuropharmacological properties of MXE. *In vitro* studies are ideally suited to provide such mechanistic insight and have a higher throughput compared with *in vivo* studies, which is a clear benefit considering that full neuropharmacological profiles are hard to obtain for the rapidly increasing numbers of NPS. Most (illicit) drugs are known to affect the function of neurotransmitter receptors and monoamine transporters (Elliot & Beveridge, 2005; Rothman and Baumann, 2003), which are therefore also endpoints of interest to investigate for MXE. Functional effects on receptors can be determined by investigating effects on the intracellular calcium concentration $[Ca^{2+}]_i$ combined with specific stimuli (e.g., acetylcholine), using single cell imaging techniques (Hondebrink et al., 2012). Effects on monoamine transporters are frequently investigated using expression models in which the transporter of interest is transfected (Verrico et al., 2007; Simmler et al., 2014; Zwartsen et al., 2017). In addition to such specific modes of action, neuronal network activity has emerged as an integrated endpoint in *in vitro* neurotoxicity testing (Johnstone et al., 2010). We have previously demonstrated in rat cortical cultures that MXE is far more potent in inhibiting neuronal network activity (IC_{50} 0.5 μM) than common drugs of abuse like amphetamine and 3,4-methylenedioxymethamphetamine (MDMA) and another NPS, 4-fluoroamphetamine (Hondebrink et al., 2016). Whether MXE is as potent in a human *in vitro* model, is currently unknown. Since *in vitro* neurotoxicity testing is shifting towards using models of human origin (Wang, 2015; Shinde et al., 2016; Schmidt et al., 2017), we selected several models of human origin, including human embryonic kidney cells (HEK293), a human neuronal cell line (SH-SY5Y), human induced pluripotent stem cell (iPSC)-derived neurons and iPSC-derived astrocytes. Since MXE is a ketamine analogue, we also investigated neuropharmacological effects of ketamine.

In summary, we investigated the effects of MXE and ketamine at pharmacologically and toxicologically relevant concentrations on the function of different neurotransmitter uptake transporters, ion channel- and neurotransmitter receptor-mediated calcium entry and spontaneous neuronal activity in different human *in vitro* models.

2. Materials and methods

2.1. Chemicals

Methoxetamine (MXE, purity >97%) was obtained from Lipomed (Weil am Rhein, Germany). Ketamine was obtained from Eurocept Pharmaceuticals. Fura-2 AM was obtained from Molecular Probes (Invitrogen, Breda, The Netherlands). Neurobasal®-A (NBA) Medium, L-glutamine, fetal bovine serum (FBS), B-27 supplement, KnockOut Serum Replacement, 50/50 DMEM/F12 medium and penicillin-streptomycin (Pen/Strep) (10,000 U/mL-10000 μg/mL) were purchased from Life Technologies (Bleiswijk, The Netherlands). iCell® Neurons Maintenance Medium (NRM-100-121-001) and iCell® Neurons Medium Supplement (NRM-100-031-001) were purchased from Cellular Dynamics International (Madison, WI, USA). All other chemicals were obtained from Sigma-Aldrich (Zwijndrecht, The Netherlands).

Stock solutions of MXE (0.1 M) and ketamine (0.1 M) were prepared in saline and stored at 4 °C for a maximum of 2 weeks. Working solutions were prepared in saline just before use. Hank's Balanced Salt Solution (1X) (HBSS) buffer solution in H_2O (cell culture grade) was prepared with addition of 20 mM HEPES.

2.2. Cell culture

All cells were cultured in a humidified 5% CO_2 atmosphere at 37 °C.

2.2.1. Rat primary cortical cells

Rat primary cortical cells were isolated from the neonatal cortex from post-natal day (PND) 1 Wistar rat pups as described previously (de Groot et al., 2016; Hondebrink et al., 2016). Briefly, rat pups were decapitated and cortices were rapidly dissected on ice. Tissues were kept in dissection medium containing NBA medium, supplemented with 25 g/L sucrose, 450 μM L-glutamine, 30 μM glutamate, 1% Pen/Strep and 10% FBS, pH was set to 7.4. Cells were

seeded in dissection medium on poly-L-lysine (50 μg/mL) coated culture materials. After 1 day in culture (DIV1), 90% of the dissection medium was replaced with comparable medium, but with 2% B-27 supplement instead of FBS. At DIV4, 90% of the medium was replaced with NBA medium, supplemented with 15 g/L sucrose, 450 μM L-glutamine, 1% Pen/Strep and 10% FBS, pH was set to 7.4 (glutamate-free medium). For Ca^{2+} imaging experiments, cortical cells were subcultured in glass-bottom dishes (MatTek, Ashland, MA) up to 14 days *in vitro* (DIV) in 2.5 mL medium at a density of $4.0*10^5$ cells/dish. Ca^{2+} imaging measurements were performed at DIV7-14, which relates to the time frame during which cortical cultures show maximal spontaneous neuronal activity (Hondebrink et al., 2016). For MEA experiments, a 50 μL drop of cell suspension ($1*10^5$ cells/well) was placed on the electrode field in each well of a 48-wells microelectrode array plate. MEA measurements were performed at DIV9-10. All animal experiments were performed in accordance with the Dutch law and were approved by the Ethical Committee for Animal Experimentation of Utrecht University. All efforts were made to treat the animals humanely and for alleviation of suffering.

2.2.2. Human SH-SY5Y cells

Human neuroblastoma SH-SY5Y cells were grown for up to 11 passages in 50/50 DMEM/F-12 medium supplemented with 15% FBS and 2% Pen/Strep. Medium was refreshed every 2–3 days. For Ca^{2+} imaging experiments, undifferentiated SH-SY5Y cells were subcultured in glass-bottom dishes at a density of $2.5–4.0*10^5$ cells/dish and Ca^{2+} imaging measurements were performed 1–2 days after seeding in glass-bottom dishes (DIV1-2).

2.2.3. Human-induced pluripotent stem cell (hiPSC)-derived iCell® neurons

iCell® neurons (NRC-100-010-001, Cellular Dynamics International (CDI), Madison, WI, USA) and iCell® astrocytes (ASC-100-020-001-PT, CDI, Madison, WI, USA) were seeded and cultured according to CDI protocol. For Ca^{2+} imaging experiments, iCell® neurons were seeded in glass-bottom dishes, coated with 0.1% polyethyleneimine (PEI) solution diluted in borate buffer (24 mM Sodium Borate/50 mM Boric Acid in Milli-Q, set to pH 8.4). The cells were seeded in Complete iCell® Neurons Maintenance Medium, supplemented with 2% iCell® Neurons Medium Supplement and 10 μg/mL laminin at a density of ~$1.5*10^5$ cells/dish as a 300 μL droplet on the glass. Cells were allowed to attach for 40 min, after which 1.5 mL of Complete iCell Maintenance Medium supplemented with laminin was added to the dish. At DIV1-3, 100% of the medium was replaced with NBA medium, supplemented with 10% KnockOut Serum Replacement and 1% Pen/Strep. Every 3–4 days, 50% of the medium was refreshed. Measurements of $[Ca^{2+}]_i$ were performed at DIV4-8 and at DIV21. For micro-electrode array (MEA) experiments, iCell® neurons were seeded as a described before (Tukker et al., 2016). Measurements were taken at DIV21.

For the co-culture of iCell® neurons/iCell® astrocytes, iCell® neurons were seeded as described above. For MEA-experiments, 48-well MEA plates (Axion Biosystems Inc., Atlanta, USA) were coated with PEI and after coating each well was pre-dotted with 10 μL of iCell® Neurons Maintenance medium with 80 μg/mL laminin. The iCell® neurons/iCell® astrocytes co-cultures were seeded according to CDI protocol. Briefly, iCell® neurons and iCell® astrocytes were seeded directly over the electrode field as a 10 μL droplet of cell suspension at a density of $1.4*10^5$ cells/μL, with $7.0*10^4$ iCell® neurons and $7.0*10^4$ astrocytes in Complete iCell® Neurons Maintenance Medium, supplemented with 2% iCell® Neurons Medium Supplement and 10 μg/mL laminin. The cell suspension droplet was allowed to attach to the electrode field for 35 min, after which 300 μL of Complete iCell® Maintenance Medium supplemented with laminin was added to each well. Every 2–3 days, 50% of the medium was refreshed. Measurements of neuronal electrical activity were taken at DIV21.

2.2.4. Human-induced pluripotent stem cell (hiPSC)-derived iCell® DopaNeurons

iCell® DopaNeurons (DNC-301-030-001, CDI, Madison, WI, USA) were seeded according to CDI protocol for both mono- and co-culture with iCell® astrocytes. For MEA-experiments, the iCell® DopaNeurons were seeded according to protocol and identical to the iCell® neurons/iCell® astrocytes co-culture described above. Measurements of neuronal electrical activity were taken at DIV21.

2.2.5. Human embryonic kidney (HEK) 293 cells

HEK293 cells stably expressing human DAT, NET or SERT and non-transfected HEK-cells were cultured as described before (Hysek et al., 2012; Zwartsen et al., 2017). Briefly, cells were cultured in DMEM high glucose, supplemented with 10% FBS, 2 mM L-glutamine, 50 U/mL – 50 μg/mL Pen/Strep, 1 mM sodium pyruvate, 1% minimum essential medium non-essential amino acids solution and 5 μL/mL geneticin selective antibiotic. Medium was refreshed every 2–4 days and cells were used for up to 10 passages.

2.3. Intracellular calcium imaging

Effects on neurotransmitters receptors were investigated using intracellular calcium imaging. We choose several receptors of interest, including those known to be affected by (illicit) drugs such as dopaminergic, serotonergic, cholinergic, glutamatergic, GABAergic and adrenergic receptors. In addition, purinergic receptors were included as targets of interest since the purinergic system can affect glutamatergic receptors (Köles et al., 2016), which are a primary target of ketamine and possibly also of the ketamine analogue MXE.

Saline solution (containing in mM: 125 NaCl, 5.5 KCl, 2.0 $CaCl_2$, 0.8 $MgCl_2$, 10.0 Hepes, 24.0 glucose and 36.5 sucrose at pH 7.3, adjusted with NaOH) and high K^+ saline solution (containing in mM: 5.5 NaCl, 100 KCl, 2.0 $CaCl_2$, 0.8 $MgCl_2$, 10.0 Hepes, 24.0 glucose, 36.5 sucrose at pH 7.3, adjusted with NaOH) were prepared with deionized water (Milli-Q, resistivity>18 MΩ-cm). Stock solutions, prepared in saline, contained 1 mM acetylcholine (ACh), 1 mM gamma-aminobutyric acid (GABA), 1 mM adenosine 5'-triphosphate (ATP), 1 mM serotonin (5-HT), 1 mM dopamine, 10 mM L-glutamic acid (glutamate), 1 mM DL-norepinephrine or 1 mM DL-epinephrine and were kept at −20 °C until use.

Changes in $[Ca^{2+}]_i$ were measured at room temperature with single cell intracellular calcium imaging using the Ca^{2+}-sensitive fluorescent ratio dye Fura-2 AM as described previously (Hondebrink et al., 2012). iCell® neurons were loaded with 5 μM Fura-2 AM for 25 min in saline, and subsequently washed with saline and left at room temperature for 20 min to allow de-esterification of Fura-2 AM. Cells were placed on the stage of an Observer A1 inverted microscope (×40 oil-immersion objective, Zeiss, Göttingen, Germany) equipped with a TILL Photonic Polychrome IV (Xenon Short Arc lamp, 150 W; TILL Photonics GmBH, Gräfelfing, Germany) and continuously superfused with saline using a Valvelink 8.2 (Automate Scientific, Berkeley, CA). After excitation at 340 (F_{340}) and 380 (F_{380}) nm wavelengths, fluorescence was collected every 3 s at 510 nm (emission) with an Image SensiCam digital camera (TILL Photonics GmBH). Each experiment consisted of a 5 min baseline recording, followed by changing superfusion to one of the stimuli used (100 mM K^+, 100 μM ACh, 1 mM ATP, 100 μM glutamate, 1 mM norepinephrine, 1 mM epinephrine, 1 mM 5-HT, 1 mM dopamine and 100 μM GABA). After an 8 min recovery period, cells were exposed to saline (control),

MXE (10 μM) or ketamine (10 μM) for 20 min. Following this 20 min, cells were stimulated again, either in the absence (control) or presence of MXE/ketamine. These experiments thus consisted of saline exposure (5 min basal recording), stimulus exposure (21 s), saline (control), MXE or ketamine exposure (20 min), stimulus (control) or stimulus + MXE/ketamine exposure (21 s). For all experiments using glutamate as stimulus, Mg^{2+} was omitted from the saline solution. All experiments were performed between DIV4-8 and at DIV21.

2.4. Multi-well microelectrode array (mwMEA) recordings

Multi-well microelectrode array (mwMEA) plates contain 48 wells per plate, with each well containing an electrode array of 16 individual embedded nanotextured gold microelectrodes with four integrated ground electrodes, yielding a total of 768 channels (Axion Biosystems Inc.). Spontaneous electrical activity was recorded as described previously (Hondebrink et al., 2016). Briefly, experiments were performed at DIV9 (rat cortical cultures) or at DIV21 (iCell® neurons, iCell® DopaNeurons, co-cultures with iCell astrocytes) at 37 °C, using a Maestro 768-channel amplifier with integrated heating system, temperature controller and data acquisition interface (Axion BioSystems Inc, Atlanta, USA). After a 5 min equilibration period, a 30 min baseline recording of the spontaneous activity was started. Only wells with at least one visibly active electrode after equilibration were included. After baseline recording, 33 μL MXE (final concentrations 0.1–100 μM, diluted in NBA medium supplemented with 10% KnockOut Serum Replacement and 1% Pen/Strep) was added to the wells (iCell® neurons, iCell® DopaNeurons, co-cultures with astrocytes). For rat cortical cultures, 5 μL MXE or ketamine (final concentrations 0.03–10 μM, diluted in FBS medium) was added to the wells and activity was recorded for another 30 min.

2.5. Monoamine transporter uptake

Uptake activity of hNET, hDAT and hSERT was measured using the Neurotransmitter Transporter Uptake Assay Kit (MDS Analytical Technologies, Sunnyvale, CA, USA) as described previously (Zwartsen et al., 2017). Briefly, HEK 293 cells were seeded in black, 96-well plates coated with poly-L-lysine at a density of $6.0*10^4$ cells/well. At DIV1, culture medium was replaced by dye solution (containing dye mix, consisting of fluorescent substrate and a masking dye, dissolved in HBSS) following 12 min pre-incubation with dye solution, 100 μL HBSS with or without MXE (final concentration 30 nM - 1 mM) was added to each well for 30 min. Fluorescence was measured at 37 °C with a microplate reader every 3 min after addition of the dye solution at 430/515 nm excitation/emission wavelength.

2.6. Data analysis and statistics

Calcium-imaging data were processed and analyzed with TILL-Vision software (version 4.01) and a custom-made MS Excel macro that calculates background-corrected ratio values (F340/F380) as described previously (Hondebrink et al., 2012). All data are expressed as mean ± SEM of n cells from N experiments (dishes). The second stimulus-evoked increase in ratio was expressed as a percentage of the first stimulus-evoked increase in ratio to derive an 'evoked treatment ratio'. The treatment ratio in control experiments was set to 100%. Effects <25% were considered irrelevant. Responding cells are cells that showed an increase in $[Ca^{2+}]_i$ during stimulus exposure ≥ 1.25 Relative Fluorescent Units (RFU). Outliers in stimulus-evoked $[Ca^{2+}]_i$ or baseline (values 2*SD above or below average) were removed from analysis (<7% and <9%, respectively). An unpaired *t*-test was used for testing the significance of the MXE-effect relative to control for stimulus-evoked effects on F340/F380 ratio (intracellular calcium concentration). Effects were considered statistically significant if $p < 0.05$.

MEA data were analyzed by NeuroExplorer5 software (NEX Technologies, Madison, USA) and custom-made MS Excel macros as described previously (Hondebrink et al., 2016). Raw data files were re-recorded for spike detection using the AxIS spike detector (Adaptive threshold crossing, Ada BandFit v2) with a threshold spike detector set at 6*SD of the internal noise level on each electrode. The re-recorded raw data were loaded into NeuroExplorer to determine the average mean spike rate (MSR; spikes/s) of all active electrodes per active well. Electrodes were considered active when MSR>0.1 spikes/s and wells were considered active when ≥1 active electrode was present. The development of spontaneous activity (MSR) over time and the effect of MXE on spontaneous activity was determined by custom-made MS Excel macros. The MSR during the exposure recording ($MSR_{exposure}$) was expressed as a percentage of the MSR during the baseline recording ($MSR_{baseline}$) to derive a treatment ratio. Treatment ratios of individual electrodes were averaged per well and subsequently per condition. Outliers (effects 2*SD above or below average) in control and effect data were excluded for further analysis (<7%). The treatment ratios in control experiments were set to 100%. Groups were compared using an ANOVA followed by a post-hoc Bonferroni test. Effects were considered statistically significant when $p < 0.05$.

For monoamine transporter uptake, data were processed and analyzed using GraphPad Prism as described previously (Zwartsen et al., 2017). All data are expressed as mean ± SEM of n wells from N plates. Uptake of the fluorescent substrate was determined per well by calculating the change in fluorescence (ΔFU) at 12 min after drug exposure compared to the fluorescence prior to exposure (i.e. following 12 min pre-incubation with the fluorescent substrate). Subsequently, ΔFU was normalized to the fluorescence prior to exposure and expressed as a percentage of control cells. Outliers in exposure groups (values 2*SD above or below average) were removed from analysis (<3%).

For all data analyses, GraphPad Prism v6.05 (GraphPad Software, San Diego, California) was used.

3. Results

3.1. Effect on receptor-mediated calcium signaling in rat primary cortical cells

Previously, several drugs have been demonstrated to affect the function of voltage-gated calcium channels and neurotransmitter receptor-mediated Ca^{2+} influx pathways (Hondebrink et al., 2012, 2011a, 2011b). We therefore investigated if MXE and ketamine at 10 μM can affect receptor-mediated calcium signaling. This MXE concentration is close to the estimated brain concentration of 1–5 μM during recreational use (Zwartsen et al., 2017). The effect of 10 μM MXE or 10 μM ketamine on depolarization (K^+)- and glutamate-mediated calcium entry was investigated. The MXE and ketamine-induced inhibition of depolarization-evoked increases in $[Ca^{2+}]_i$ was insignificant (Fig. 1A, C). However, MXE significantly augments the glutamate-evoked increase in $[Ca^{2+}]_i$ to 123 ± 7%, whereas the effect of ketamine on the glutamate-evoked increase in $[Ca^{2+}]_i$ was insignificant (Fig. 1B and C). In addition, exposure of rat cortical cells to 10 μM MXE was without effects on ACh-, ATP, or epinephrine-mediated calcium entry (not shown).

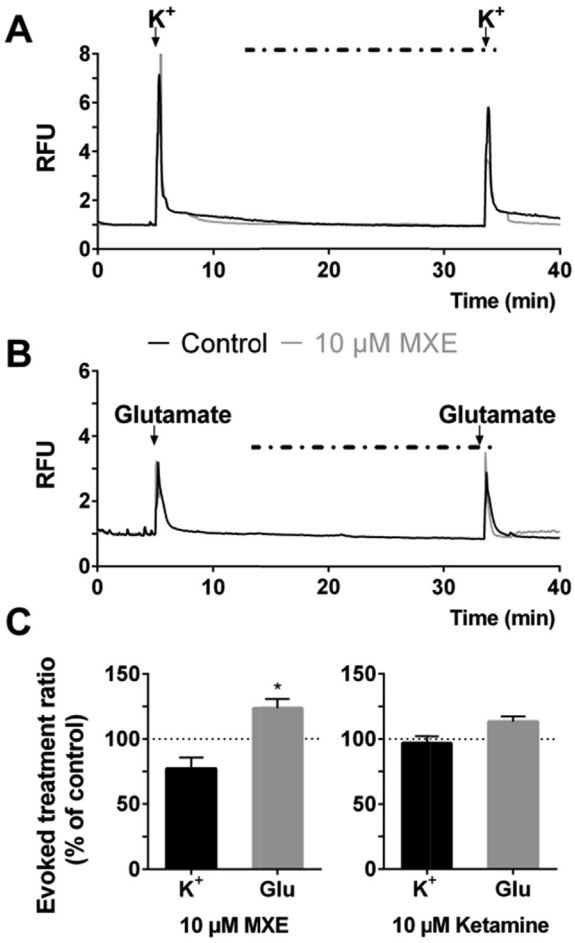

Fig. 1. Effects of MXE and ketamine on the stimulus-evoked increase in $[Ca^{2+}]_i$ in rat primary cortical cells. Representative recordings of $[Ca^{2+}]_i$ from individual cells exposed for 20 min (dotted line above recording) to saline (black trace) or 10 μM MXE (grey trace) in between two 21 s stimulations with 100 mM K^+ (A) or 100 μM glutamate (B), as indicated by the arrows above the recording. Bar graphs of effects of MXE (C, left) or ketamine (C, right) on the increase in $[Ca^{2+}]$ evoked by K^+ (100 mM) or glutamate (100 μM; Glu). Data (mean + SEM) are presented as the treatment ratio of drug-exposed cells as a percentage of saline-exposed cells. n_{cells} = 16–26, $N_{experiments}$ = 3–4; *$p < 0.05$ vs control.

3.2. Effect on neuronal electrical activity in rat primary cortical cells

Rat cortical cells were cultured on mwMEAs for up to 10 days to test effects of MXE and ketamine on spontaneous neuronal activity as an integrated endpoint. We have previously shown that MXE potently inhibits neuronal activity in primary rat cortical cultures, with an IC_{50} of 0.5 μM (Hondebrink et al., 2016). For intra-laboratory comparison, the effect of MXE on neuronal activity in rat cortical cultures was measured again, yielding comparable results. MXE concentration-dependently inhibited neuronal activity with an IC_{50} of 0.5 μM (Fig. 2), clearly indicating the reproducibility of mwMEA recordings. Ketamine also inhibited neuronal activity concentration-dependently, with an IC_{50} of 1.2 μM (Fig. 2). At 1 μM, neuronal activity was more potently inhibited by MXE (to 27%) compared to ketamine (to 62%) ($p < 0.05$).

3.3. Effect on receptor-mediated calcium signaling in human in vitro models

3.3.1. SY-SY5Y cells

Human SH-SY5Y cells were challenged with K^+-, ACh-, glutamate-, GABA-, norepinephrine-, epinephrine-, 5-HT-, dopamine- and ATP-containing saline to determine the presence of functional neurotransmitter pathways. Depolarization (100 mM K^+) and ACh (100 μM) evoked transient increases in $[Ca^{2+}]_i$ that amounted to respectively 3.1 ± 0.1 and 4.8 ± 0.1 RFU. However, stimulation with glutamate (100 μM), GABA (100 μM), epinephrine (1 mM), 5-HT (1 mM), dopamine (1 mM) or ATP (1 mM) did not result in detectable increases in $[Ca^{2+}]_i$.

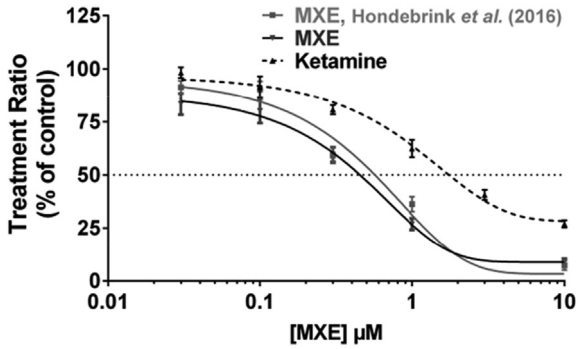

Fig. 2. MXE- and ketamine-induced effects on neuronal electrical activity in rat cortical cultures. Data (mean ± SEM) are presented as the evoked treatment ratio of drug-exposed wells as a percentage of saline-exposed wells (change in % between $MSR_{baseline}$ and $MSR_{exposure}$, relative to control wells). Data were synchronized to the time of exposure. The dotted line indicates 50% inhibition. n_{wells} = 14–20, N_{plates} = 2–3.

We therefore used SH-SY5Y cells only to investigate the effect of MXE on depolarization- (K^+) and ACh-mediated calcium entry. MXE (10 μM) induced a modest but significant inhibition of both the K^+- and ACh-evoked increases in $[Ca^{2+}]_i$ of 20± 4% and 8 ± 2%, respectively (Fig. 3).

3.3.2. Human-induced pluripotent stem cell (hiPSC)-derived iCell® neurons

hiPSC iCell® neurons were challenged with K^+-, ACh-, glutamate-, GABA-, norepinephrine-, epinephrine-, 5-HT-, dopamine- and ATP-containing saline to determine the presence of functional neurotransmitter receptor pathways. Stimulation with norepinephrine-, epinephrine-, 5-HT-, or dopamine-containing saline did not result in detectable increases in $[Ca^{2+}]_i$. However, depolarization (100 mM K^+), ACh (100 μM), glutamate (100 μM) and ATP (1 mM) evoked transient increases in $[Ca^{2+}]_i$. GABA (100 μM), which is the main inhibitory input in the adult brain, appeared to be excitatory early in culture (DIV4-8), but not in more mature cultures (DIV21). Therefore, mature cultures could not be used to measure effects of MXE on GABA-evoked calcium signaling and experiments were performed at DIV4-8.

MXE (10 μM) significantly inhibited the ATP-evoked increase in

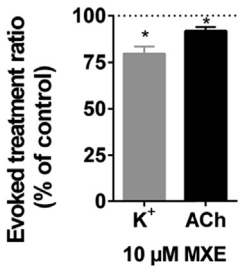

Fig. 3. Effects of MXE on the stimulus-evoked increase in $[Ca^{2+}]_i$ in human SH-SY5Y cells. Cells were exposed for 20 min to saline or 10 μM MXE in between two 21s stimulations with K^+ (100 mM) or acetylcholine (100 μM; ACh). Data (mean + SEM) are presented as the evoked treatment ratio of drug-exposed cells as a percentage of saline-exposed cells. n_{cells} = 86–129, $N_{experiments}$ = 15–19; *p < 0.05 vs control.

$[Ca^{2+}]_i$ (79 ± 6% of control, $p < 0.01$, Fig. 4B and C), whereas the K^+-, ACh-, Glu- and GABA-evoked increases in $[Ca^{2+}]_i$ were not affected compared with control (Fig. 4A, C).

3.4. Effect on neuronal electrical activity

Since MXE potently inhibited spontaneous neuronal activity in rat primary cortical cells (IC_{50} 0.5 μM, Fig. 2), the effect of MXE on neuronal activity in different human iPSC-derived neuronal models was investigated. iCell® neurons are primarily composed of post-mitotic glutamatergic and GABAergic neurons (Tukker et al., 2016), thereby resembling cortical neurons. We also measured the effect of MXE on neuronal activity in human iPSC-derived dopaminergic iCell® DopaNeurons, which represent fully differentiated midbrain dopaminergic neurons. Both models (iCell® neurons and iCell® DopaNeurons) represent pure neuronal cultures without astrocytes. Therefore, both models were also grown as co-culture with hiPSC-derived astrocytes to better represent the *in vivo* brain.

In both iCell® neuronal cultures and co-cultures with astrocytes, exposure to 1 μM MXE did not affect neuronal activity. In iCell® pure neuronal cultures, exposure to 10 μM MXE decreased neuronal activity significantly to 68 ± 6% ($p < 0.05$ vs control; Fig. 5A), whereas in co-cultures with astrocytes, exposure to 10 μM MXE decreased neuronal activity significantly to 41 ± 9% ($p < 0.05$ vs control; Fig. 5B). The decrease in neuronal activity following exposure to 10 μM MXE in the presence of astrocytes (Fig. 5B) was not significantly lower than in the absence of astrocytes (Fig. 5A). Exposure to 100 μM MXE almost completely abolished neuronal activity in both types of cultures ($p < 0.05$ vs control; Fig. 5A and B), although this concentration is well above the estimated brain concentration during recreational use and may thus be of limited pharmacological relevance.

In iCell® DopaNeurons monocultures, only 100 μM MXE significantly inhibited neuronal activity to 5 ± 1% ($p < 0.05$ vs control; Fig. 5C). In co-cultures with astrocytes, both 10 and 100 μM MXE inhibited neuronal activity significantly to 77 ± 4% and 14 ± 2%, respectively ($p < 0.05$ vs control; Fig. 5D).

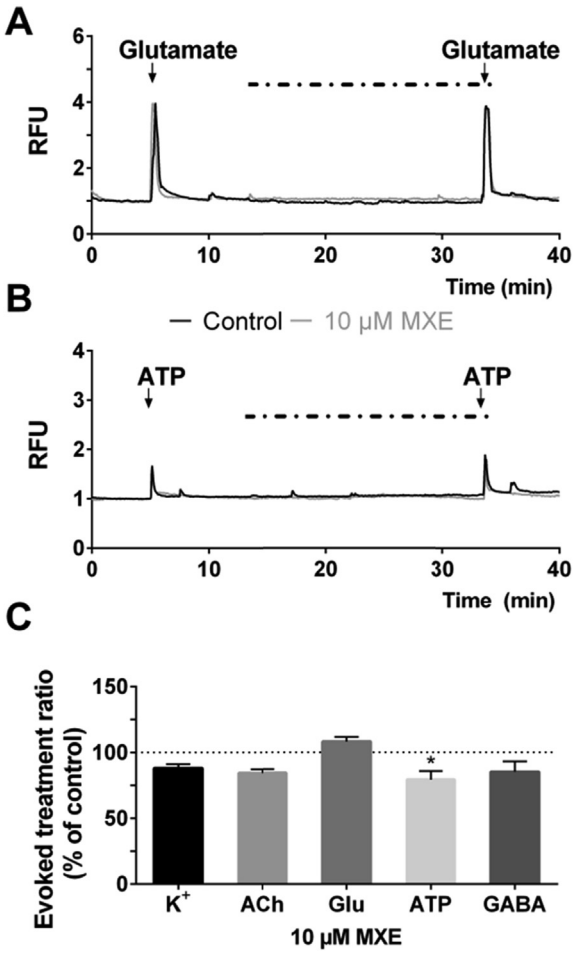

Fig. 4. Effects of MXE on the stimulus-evoked increase in $[Ca^{2+}]_i$ in hiPSC neurons. Representative recordings of $[Ca^{2+}]_i$ from individual iCell® neurons exposed for 20 min (dotted line above recording) to saline (black trace) or 10 μM MXE (grey trace) in between two 21 s stimulations with 100 μM glutamate (A) or 1 mM ATP (B), as indicated by the arrows above the recording. (C) Bar graphs of effects of MXE on the increase in $[Ca^{2+}]_i$ evoked by K^+ (100 mM), acetylcholine (100 μM; ACh), glutamate (100 μM; Glu), ATP (1 mM) or GABA (100 μM). Data (mean + SEM) are presented as the treatment ratio of drug-exposed cells as a percentage of saline-exposed cells. $n_{cells} = 8–148$, $N_{experiments} = 2–14$; $^*p < 0.05$ vs control.

3.5. Inhibition of monoamine transporter uptake

Since drugs of abuse commonly interfere with monoamine uptake transporters, we investigated the effect of MXE on different human monoamine transporters expressed in HEK293 cells. The uptake of fluorescent substrate by hDAT, hNET and hSERT was measured following exposure to MXE. MXE inhibited the uptake of fluorescent substrate via monoamine transporters concentration-dependently (Fig. 6). MXE was equipotent for hDAT and hNET, with IC_{50} values of 33 and 20 μM, respectively, whereas MXE was ten times more potent for hSERT, with an IC_{50} value of 2 μM.

4. Discussion

We investigated the pharmacological profile of the two structurally comparable substances MXE and ketamine. Ketamine (10 μM) did not affect the K^+- or glutamate-evoked increase in $[Ca^{2+}]_i$ in rat cortical cultures, but potently inhibited spontaneous neuronal activity. Although ketamine has previously been reported to inhibit e.g. NMDA- and nicotinic ACh-receptors and L-type Ca^{2+} channels (Coates and Flood, 2001; Hatakeyama et al., 2001; Parsons et al., 1996; Yamakage et al., 1995; Yamakura et al., 1993, 2000), these effects are frequently observed at higher concentrations. On the other hand, MXE slightly enhanced the glutamate-evoked increase in $[Ca^{2+}]_i$, but only in the rat cortical culture. This increase in glutamate-evoked $[Ca^{2+}]_i$ following MXE exposure was not observed in human neuronal cultures. Notably, MXE inhibited neuronal electrical activity in human neuronal cultures, both in mono- and co-culture with astrocytes, although less potently compared to the inhibition observed in rat cortical cultures. Finally, MXE potently inhibited hSERT and to a lesser extent hDAT and hNET. Most effects were observed at relevant MXE concentrations, i.e. close to or within the range of the estimated brain concentration during recreational use (1–5 μM; Zwartsen et al., 2017).

In rat cortical cultures, MXE modestly increased the glutamate-evoked increase in $[Ca^{2+}]_i$, but strongly decreased neuronal activity. Likely, these seemingly conflicting observations are due to a dominant inhibitory component of the neuronal network used for measurements of neuronal activity. We have previously shown that (over)excitation of the network often manifests as an inhibition of neuronal activity in MEA recordings. For example, exposure to high concentrations of glutamate or to excitatory chemicals, such as pyrethroid- and organophosphorus insecticides, decreases neuronal activity (Dingemans et al., 2016; Hondebrink et al., 2016; Meyer et al., 2008; Tukker et al., 2016; Vassallo et al., 2016), despite the clear excitatory effects of these substances on individual cells.

Although MEA recordings of neuronal activity are very suitable to screen for drug effects, they are less suitable to pinpoint the exact

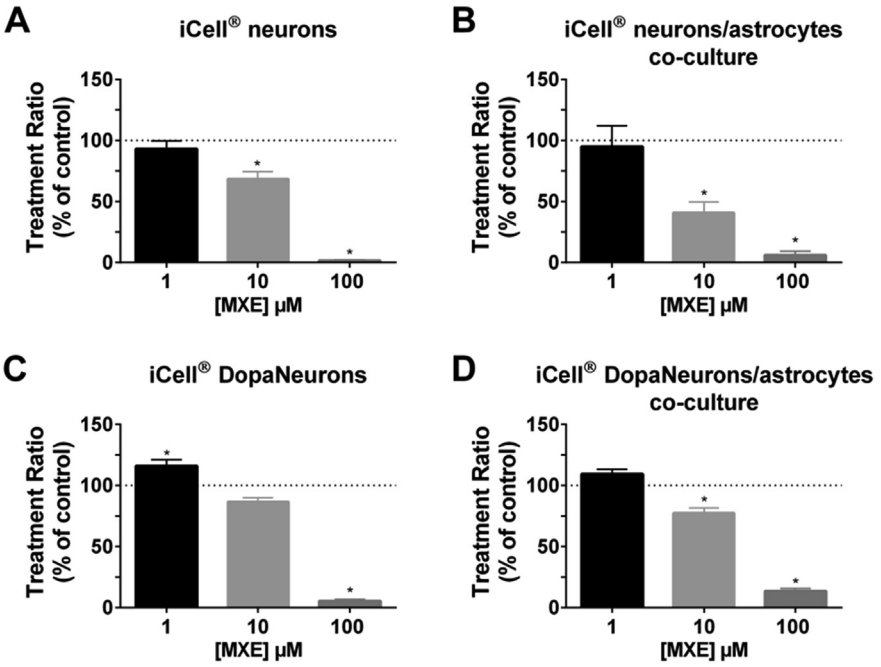

Fig. 5. MXE-induced effects on neuronal electrical activity in human iPSC-derived iCell® neurons (A), iCell® neurons in co-culture with astrocytes (B), iCell® DopaNeurons (C) and iCell® DopaNeurons in co-culture with astrocytes (D). Data (mean ± SEM) are presented as the evoked treatment ratio of drug-exposed wells as a percentage of saline-exposed wells (change in % between $MSR_{baseline}$ and $MSR_{exposure}$, relative to control wells). Data were synchronized to the time of exposure. $n_{wells} = 8–14$, $N_{plates} = 2–4$; $^{*}p < 0.05$ vs control.

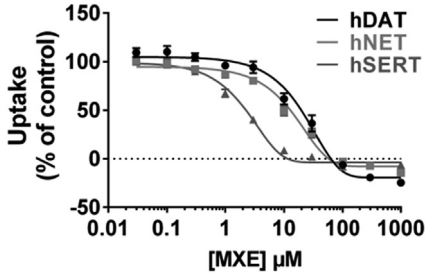

Fig. 6. Concentration-effect curve of uptake via human monoamine transporters following exposure to MXE. MXE inhibits uptake of fluorescent substrate by hDAT, hNET and hSERT. Data (mean ± SEM) are expressed as percentage of saline-exposed controls. n = 14–16, N = 4.

underlying (individual) mechanisms. For example, addition of specific glutamate receptor (AMPA, kainate and-or NMDA) antagonists (completely) inhibits neuronal activity (Hondebrink et al., 2016). As a result, additional effects of substances on neuronal activity cannot be measured using MEA recordings, hampering mechanistic investigation of MXE effects.

MXE strongly inhibited neuronal activity, both in rat cortical cultures and human iPSC-derived neuronal cultures with astrocytes (Figs. 2 and 5). Since astrocytes can have protective effects on neuronal function (Sofroniew, 2005), we also measured effects of MXE on neuronal activity in human iCell® neurons in the absence of astrocytes. No significant differences in MXE effects were observed between pure neuronal cultures and co-cultures with astrocytes, for both iCell® neurons and iCell® DopaNeurons (Fig. 5). This suggests that astrocytes are not an important target in MXE-induced neuropharmacological effects.

Interestingly, the MEA data show that the rat cortical cultures are more sensitive to MXE than the human iPSC-derived pure neuronal cultures and co-cultures with astrocytes. This may indicate that the rat cortical cultures are too sensitive to MXE when compared with the human *in vivo* situation or that iCell® (Dopa) neurons are not sensitive enough. Data from other chemicals (MeHg, CNQX/MK801 and bicuculline) show an approximately comparable difference in sensitivity between the rat cortical cultures and iCell® neuron monocultures (unpublished). Whether these differences in sensitivity are related to the relatively immature phenotype of iCell® neurons (Odawara et al., 2016) and/or differences in receptor expression or isoforms remains to be determined. On the other hand, toxins like TTX (Kasteel and Westerink, 2017) and drugs like amphetamine (Hondebrink et al., 2016; Tukker et al., 2016) indicate a comparable sensitivity for human iCell® neurons and primary rat cortical cultures.

We also showed that MXE inhibits hSERT, hNET and hDAT at low µM concentrations (IC_{50} values of 2, 20 and 33 µM respectively), in line with Roth et al. (2013) who showed a Ki value for hSERT of 0.4 µM and no binding affinity for hNET up to 10 µM MXE. MXE is more potent in inhibiting monoamine transporters than ketamine, which did not show binding affinity for hSERT and hNET up to 10 µM (Roth et al., 2013) and a Ki value for hNET of 67 µM (Nishimura et al., 1998). In addition, ketamine was also less potent than MXE in inhibiting uptake by rat DAT and SERT, with Ki values for ketamine of respectively 63 and 162 µM.

This is one of the first studies that investigated the neuropharmacological profile of MXE and reports effects on functional endpoints such as neuronal activity and transporter activity. We showed that the use of different (neuronal) endpoints assessed in multiple *in vitro* models can be complementary for pharmacological profiling. Since the number of NPS is continuously increasing, rapid *in vitro* screening methods as those presented here could proof of utmost importance for gaining a first mechanistic insight to aid the risk assessment of emerging NPS.

Conflict of interest

The authors do not have any conflict of interest.

Acknowledgements

We gratefully acknowledge the members of the Neurotoxicology Research Group for helpful discussions and Dr. Hoener from F. Hoffmann-La Roche Ltd (Basel, Switzerland) for supplying the transfected HEK cells. This work was supported by the Dutch Poisons Information Center (DPIC; University Medical Center Utrecht), the National Centre for the Replacement, Refinement and Reduction of Animals in Research (NC3Rs; project number 50308-372160) and the Faculty of Veterinary Medicine (Utrecht University).

References

Bergman, S.A., 1999. Ketamine: review of its pharmacology and its use in pediatric anesthesia. Anesth. Prog. 46, 10–20.

Coates, K.M., Flood, P., 2001. Ketamine and its preservative, benzethonium chloride, both inhibit human recombinant alpha7 and alpha4beta2 neuronal nicotinic acetylcholine receptors in Xenopus oocytes. Br. J. Pharmacol. 134, 871–879. http://dx.doi.org/10.1038/sj.bjp.0704315.

Corazza, O., Assi, S., Schifano, F., 2013. From "Special K" to "Special M": the evolution of the recreational use of ketamine and methoxetamine. CNS Neurosci. Ther. 19, 454–460. http://dx.doi.org/10.1111/cns.12063.

Corazza, O., Schifano, F., Simonato, P., Fergus, S., Assi, S., Stair, J., Corkery, J., Trincas, G., Deluca, P., Davey, Z., Blaszko, U., Demetrovics, Z., Moskalewicz, J., Enea, A., di Melchiorre, G., Mervo, B., di Furia, L., Farre, M., Flesland, L., Pasinetti, M., Pezzolesi, C., Pisarska, A., Shapiro, H., Siemann, H., Skutle, A., Enea, A., di Melchiorre, G., Sferrazza, E., Torrens, M., van der Kreeft, P., Zummo, D., Scherbaum, N., 2012. Phenomenon of new drugs on the Internet: the case of ketamine derivative methoxetamine. Hum. Psychopharmacol. 27, 145–149. http://dx.doi.org/10.1002/hup.1242.

Dargan, P.I., Tang, H.C., Liang, W., Wood, D.M., Yew, D.T., 2014. Three months of methoxetamine administration is associated with significant bladder and renal toxicity in mice. Clin. Toxicol. 52, 176–180. http://dx.doi.org/10.3109/15563650.2014.892605.

de Groot, M.W.G.D.M., van Kleef, R.G.D.M., de Groot, A., Westerink, R.H.S., 2016. In vitro developmental neurotoxicity following chronic exposure to 50 Hz extremely low-frequency electromagnetic fields in primary rat cortical cultures. Toxicol. Sci. 149, 433–440. http://dx.doi.org/10.1093/toxsci/kfv242.

Dingemans, M.M.L., Schütte, M.G., Wiersma, D.M.M., de Groot, A., van Kleef, R.G.D.M., Wijnolts, F.M.J., Westerink, R.H.S., 2016. Chronic 14-day exposure to insecticides or methylmercury modulates neuronal activity in primary rat cortical cultures. Neurotoxicology 57, 194–202. http://dx.doi.org/10.1016/j.neuro.2016.10.002.

Elliott, J.M., Beveridge, T.J., 2005. Psychostimulants and monoamine transporters: upsetting the balance. Curr. Opin. Pharmacol. 5 (1), 94–100.

EMCDDA, 2016. European Drug Report 2016: Trends and Developments. http://dx.doi.org/10.2810/04312.

EMCDDA, Europol, 2014. EMCDDA | EMCDDA–Europol Joint Report on a New Psychoactive Substance: Methoxetamine (2-(3-methoxyphenyl)-2-(ethylamino)cyclohexanone). http://dx.doi.org/10.2810/28543.

Europol, 2013. EU Drugs Markets Report: a Strategic Analysis. http://dx.doi.org/10.2810/85143.

van der Gouwe, D., 2014. DIMS Jaarbericht 2014. Trimbos Institute. Accessed via. https://assets.trimbos.nl/docs/dcd6beec-29e2-4488-b76f-3118f74b8643.pdf.

Hatakeyama, N., Yamazaki, M., Shibuya, N., Yamamura, S., Momose, Y., 2001. Effects of ketamine on voltage-dependent calcium currents and membrane potentials in single bullfrog atrial cells. J. Anesth. 15 (3), 149–153. http://dx.doi.org/10.1007/S005400170017.

Hondebrink, L., Meulenbelt, J., Meijer, M., Van Den Berg, M., Westerink, R.H.S., 2011a. High concentrations of MDMA ('ecstasy') and its metabolite MDA inhibit calcium influx and depolarization-evoked vesicular dopamine release in PC12 cells. Neuropharmacology 61, 202–208. http://dx.doi.org/10.1016/j.neuropharm.2011.03.028.

Hondebrink, L., Meulenbelt, J., van Kleef, R.G.D.M., van den Berg, M., Westerink, R.H.S., 2011b. Modulation of human GABAA receptor function: a novel mode of action of drugs of abuse. Neurotoxicology 32, 823–827. http://dx.doi.org/10.1016/j.neuro.2011.05.016.

Hondebrink, L., Meulenbelt, J., Rietjens, S.J., Meijer, M., Westerink, R.H.S., 2012. Methamphetamine, amphetamine, MDMA ('ecstasy'), MDA and mCPP modulate electrical and cholinergic input in PC12 cells. Neurotoxicology 33, 255–260. http://dx.doi.org/10.1016/j.neuro.2011.09.003.

Hondebrink, L., Nugteren-van Lonkhuyzen, J.J., van Der Gouwe, D., Brunt, T.M., 2015. Monitoring new psychoactive substances (NPS) in The Netherlands: data from the drug market and the poisons information centre. Drug Alcohol Depend. 147, 109–115. http://dx.doi.org/10.1016/j.drugalcdep.2014.11.033.

Hondebrink, L., Verboven, A.H.A., Drega, W.S., Schmeink, S., de Groot, M.W.G.D.M., van Kleef, R.G.D.M., Wijnolts, F.M.J., de Groot, A., Meulenbelt, J., Westerink, R.H.S., 2016. Neurotoxicity screening of (illicit) drugs using novel methods for analysis of microelectrode array (MEA) recordings. Neurotoxicology 55, 1–9. http://dx.doi.org/10.1016/j.neuro.2016.04.020.

Horsley, R.R., Lhotkova, E., Hajkova, K., Jurasek, B., Kuchar, M., Palenicek, T., 2016. Detailed pharmacological evaluation of methoxetamine (MXE), a novel psychoactive ketamine analogue—Behavioural, pharmacokinetic and metabolic studies in the Wistar rat. Brain Res. Bull. http://dx.doi.org/10.1016/j.brainresbull.2016.05.002.

Hysek, C.M., Simmler, L.D., Nicola, V.G., Vischer, N., Donzelli, M., Krähenbühl, S., Grouzmann, E., Huwyler, J., Hoener, M.C., Liechti, M.E., 2012. Duloxetine inhibits effects of MDMA ("ecstasy") in vitro and in humans in a randomized placebo-controlled laboratory study. PLoS One 7, e36476. http://dx.doi.org/10.1371/journal.pone.0036476.

Johnstone, A.F.M., Gross, G.W., Weiss, D.G., Schroeder, O.H.U., Gramowski, A., Shafer, T.J., 2010. Microelectrode arrays: a physiologically based neurotoxicity testing platform for the 21st century. Neurotoxicology. http://dx.doi.org/10.1016/j.neuro.2010.04.001.

Kasteel, E.E.J., Westerink, R.H.S., 2017. Comparison of the acute inhibitory effects of Tetrodotoxin (TTX) in rat and human neuronal networks for risk assessment purposes. Toxicol. Lett. 270, 12–16. http://dx.doi.org/10.1016/j.toxlet.2017.02.014.

Köles, L., Kató, E., Hanuska, A., Zádori, Z.S., Al-Khrasani, M., Zelles, T., Rubini, P., Illes, P., 2016. Modulation of excitatory neurotransmission by neuronal/glial signalling molecules: interplay between purinergic and glutamatergic systems. Purinergic Signal 12, 1–24. http://dx.doi.org/10.1007/s11302-015-9480-5.

Lawn, W., Borschmann, R., Cottrell, A., Winstock, A., 2014. Methoxetamine: prevalence of use in the USA and UK and associated urinary problems. J. Subst. Use 1–6. http://dx.doi.org/10.3109/14659891.2014.966345.

Linsen, F., Koning, R.P.J., van Laar, M., Niesink, R.J.M., Koeter, M.W., Brunt, T.M., 2015. 4-Fluoroamphetamine in The Netherlands: more than a one-night stand. Addiction 110, 1138–1143. http://dx.doi.org/10.1111/add.12932.

Meyer, D.A., Carter, J.M., Johnstone, A.F.M., Shafer, T.J., 2008. Pyrethroid modulation of spontaneous neuronal excitability and neurotransmission in hippocampal neurons in culture. Neurotoxicology 29, 213–225. http://dx.doi.org/10.1016/j.neuro.2007.11.005.

Nishimura, M., Sato, K., Okada, T., Yoshiya, I., Schloss, P., Shimada, S., Tohyama, M., 1998. Ketamine inhibits monoamine transporters expressed in human embryonic kidney 293 cells. Anesthesiology 88, 768–774.

Odawara, A., Katoh, H., Matsuda, N., Suzuki, I., 2016. Physiological maturation and drug responses of human induced pluripotent stem cell-derived cortical neuronal networks in long-term culture. Sci. Rep. 6, 26181. http://dx.doi.org/10.1038/srep26181.

Parsons, C.G., Panchenko, V.A., Pinchenko, V.O., Tsyndrenko, A.Y., Krishtal, O.A., 1996. Comparative patch-clamp studies with freshly dissociated rat hippocampal and striatal neurons on the NMDA receptor antagonistic effects of amantadine and memantine. Eur. J. Neurosci. 8, 446–454.

Roth, B.L., Gibbons, S., Arunotayanun, W., Huang, X.-P., Setola, V., Treble, R., Iversen, L., 2013. The ketamine analogue methoxetamine and 3- and 4-methoxy analogues of phencyclidine are high affinity and selective ligands for the glutamate NMDA receptor. PLoS One 8, e59334. http://dx.doi.org/10.1371/journal.pone.0059334.

Rothman, R.B., Baumann, M.H., 2003. Monoamine transporters and psychostimulant drugs. Eur. J. Pharmacol. 479 (1–3), 23–40.

Shinde, V., Sureshkumar, P., Sotiriadou, I., Hescheler, J., Sachinidis, A., 2016. Human embryonic and induced pluripotent stem cell based toxicity testing models: future applications in new drug discovery. Curr. Med. Chem. 23 (30), 3495–3509.

Simmler, L.D., Rickli, A., Hoener, M.C., Liechti, M.E., 2014. Monoamine transporter and receptor interaction profiles of a new series of designer cathinones. Neuropharmacology 79, 152–160.

Schmidt, B.Z., Lehmann, M., Gutbier, S., Nembo, E., Noel, S., Smirnova, L., Forsby, A., Hescheler, J., Avci, H.X., Hartung, T., Leist, M., Kobolák, J., Dinnyés, A., 2017. In vitro acute and developmental neurotoxicity screening: an overview of cellular platforms and high-throughput technical possibilities. Arch. Toxicol. 91 (1), 1–33. http://dx.doi.org/10.1007/s00204-016-1805-9.

Sofroniew, M.V., 2005. Reactive astrocytes in neural repair and protection. Neuroscience 11 (5), 400–407.

Tukker, A.M., Groot, M.W.G.D.M., De Wijnolts, F.M.J., Emma, E.J., Hondebrink, L., Westerink, R.H.S., 2016. Is the time right for in vitro neurotoxicity testing using human iPSC-derived neurons. ALTEX 33, 261–271. http://dx.doi.org/10.14573/altex.1510091.

Vassallo, A., Chiappalone, M., De Camargos Lopes, R., Scelfo, B., Novellino, A., Defranchi, E., Palosaari, T., Weisschu, T., Ramirez, T., Martinoia, S., Johnstone, A.F.M., Mack, C.M., Landsiedel, R., Whelan, M., Bal-Price, A., Shafer, T.J., 2016. A multi-laboratory evaluation of microelectrode array-based measurements of neural network activity for acute neurotoxicity testing. Neurotoxicology. http://dx.doi.org/10.1016/j.neuro.2016.03.019.

Verrico, C.D., Miller, G.M., Madras, B.K., 2007. MDMA (Ecstasy) and human dopamine, norepinephrine, and serotonin transporters: implications for MDMA-induced neurotoxicity and treatment. Psychopharmacol. Berl. 189 (4), 489–503.

Wang, C., 2015. Application of in vitro models in developmental neurotoxicity and pharmaceutics research. J. Mol. Pharm. Org. Process Res. 3, e122. http://dx.doi.org/10.4172/2329-9053.1000e122.

Yamakage, M., Hirshman, C.A., Croxton, T.L., 1995. Inhibitory effects of thiopental, ketamine, and propofol on voltage-dependent Ca^{2+} channels in porcine tracheal smooth muscle cells. Anesthesiology 83, 1274–1282. http://dx.doi.org/10.1097/00000542-199512000-00018.

Yamakura, T., Mori, H., Masaki, H., Shimoji, K., Mishina, M., 1993. Different sensitivities of NMDA receptor channel subtypes to non-competitive antagonists. Neuroreport 4, 687–690.

Yamakura, T., Chavez-Noriega, L.E., Harris, R.A., 2000. Subunit-dependent inhibition of human neuronal nicotinic acetylcholine receptors and other ligand-gated ion channels by dissociative anesthetics ketamine and dizocilpine. Anesthesiology 92, 1144–1153. http://dx.doi.org/10.1097/00000542-200004000-00033.

Zanda, M.T., Fadda, P., Chiamulera, C., Fratta, W., Fattore, L., 2016. Methoxetamine, a novel psychoactive substance with serious adverse pharmacological effects: a review of case reports and preclinical findings. Behav. Pharmacol. 1–8. http://dx.doi.org/10.1097/FBP.0000000000000241.

Zawilska, J.B., 2014. Methoxetamine – a novel recreational drug with potent hallucinogenic properties. Toxicol. Lett. 230, 402–407. http://dx.doi.org/10.1016/j.toxlet.2014.08.011.

Zwartsen, A., Verboven, A.H.A., van Kleef, R.G.D.M., Wijnolts, F.M.J., Westerink, R.H.S., Hondebrink, L., 2017. Measuring inhibition of monoamine reuptake transporters by new psychoactive substances in real-time using a high-throughput, fluorescence-based assay. Toxicol. In Vitro (in press). http://dx.doi.org/10.1016/j.tiv.2017.05.010.